A modified two-leaf light use efficiency model for improving the simulation of GPP using a radiation scalar

Xiaobin Guan [a,b], Jing M. Chen [b,c,*], Huanfeng Shen [a,d], Xinyao Xie [e]

[a] *School of Resource and Environmental Sciences, Wuhan University, Wuhan 430079, China*
[b] *Department of Geography and Planning, University of Toronto, Toronto ON M5S3G3, Canada*
[c] *School of Geographical Sciences, Fujian Normal University, Fuzhou 350117, China*
[d] *Collaborative Innovation Center of Geospatial Technology, Wuhan 430079, China*
[e] *Institute of Mountain Hazards and Environment, Chinese Academy of Sciences, Chengdu 610041, China*

A B S T R A C T

Two-leaf light use efficiency (TL-LUE) models are efficient methods to simulate regional and global gross primary productivity (GPP). A TL-LUE model has previously been shown to outperform the big-leaf MOD17 model through separate consideration of the contributions of sunlit and shaded leaves. However, the impacts of radiation intensity on LUE are inadequately considered in the TL-LUE model, and the maximum LUEs of sunlit and shaded leaves are assigned as different constants, which often induce large uncertainties. Therefore, a TL-LUE model modified with a radiation scalar (RTL-LUE) is developed in this paper. The same maximum LUE is used for both sunlit and shaded leaves, and the difference in LUE between sunlit and shaded leaf groups is determined by the same radiation scalar. The RTL-LUE model was calibrated and validated at global 169 FLUXNET eddy covariance (EC) sites. Results indicate that although GPP simulations from the TL-LUE model match well with the EC GPP, the RTL-LUE model can further improve the simulation, for half-hour, 8-day, and yearly time scales. The TL-LUE model tends to overestimate GPP under conditions of high incoming photosynthetically active radiation (PAR), because the radiation-independent LUE values for both sunlit and shaded leaves are only suitable for low-medium (e.g., average) incoming PAR conditions. The errors in the RTL-LUE model show lower sensitivity to PAR, and its GPP simulations can better track the diurnal and seasonal variations of EC GPP by alleviating the overestimation at noon and growing seasons associated with the TL-LUE model. This study demonstrates the necessity of considering a radiation scalar in GPP simulation in LUE models even if the first-order effect of radiation is already considered through differentiating sunlit and shaded leaves. The simple RTL-LUE developed in this study would be a useful alternative to complex process-based models for global carbon cycle research.

1. Introduction

Gross primary productivity (GPP), the integral of vegetation photosynthesis by all leaves at the ecosystem scale, is an important component for the terrestrial ecosystem carbon cycle (Beer et al., 2010; Chen et al., 2019b). GPP represents the total amount of atmospheric carbon dioxide fixed by vegetation per unit of space and time, and thus plays a critical role in quantifying the status and changes of the global carbon budget (Falkowski et al., 2000; Marcott et al., 2014). Under the background of the rapid global change, it is of great significance to accurately quantify GPP at regional or global scales, in order to advance our understanding of the interactions between terrestrial ecosystems and changes in atmospheric CO_2, temperature, and other variables (Xia et al., 2015; Yang et al., 2013).

In the past decades, numerous models with various complexities and structures have been developed to simulate GPP at the regional or global scale, mainly including process-based models and light use efficiency (LUE) models (Marshall et al., 2018; Yuan et al., 2014). Among them, LUE models are favored in many applications due to their simple model structure and input requirement, making the models easy to use relative to process-based models, which require large numbers of prescribed parameters and input datasets (Dong et al., 2015; Mattos et al., 2020). LUE models can be conveniently driven by the remote sensing vegetation index (VI) data, which are available globally at various resolutions (Guan et al., 2019; Xiao et al., 2010; Zhang et al., 2017). Based on the assumption that GPP linearly increases with the canopy absorbed

photosynthetically active radiation (APAR), a variety of big-leaf LUE models were developed, such as the MOD17 model (Running et al., 2004), the eddy covariance (EC-LUE) model (Yuan et al., 2007), the Vegetation Photosynthesis Model (VPM) (Xiao et al., 2004), and the Carnegie-Ames-Stanford Approach (CASA) (Potter et al., 1993). The main disparity of these models concentrates on the calculation of APAR and environmental scalars used to constrain the actual LUE departing from the optimum LUE (McCallum et al., 2013; Zhang et al., 2015).

These big-leaf LUE models treat the entire vegetation canopy as a big extended leaf, assuming that the direct and diffuse radiation are absorbed without differences in their use for photosynthesis (Haxeltine and Prentice, 1996; Wang and Leuning, 1998). However, the photosynthesis rates of sunlit and shaded leaves in plant canopies are respectively limited by the maximum carboxylation rate and the electron transport rate, and hence have different LUE values (Chen et al., 1999; De Pury and Farquhar, 1997; Propastin et al., 2012). Different groups of leaves (sunlit and shaded) have different levels of exposure to sunlight, due to their different positions in the canopy (Liu et al., 1997; Oliphant et al., 2011). Sunlit leaves absorb both direct and diffuse radiation, which are easily light-saturated. In contrast, shaded leaves can only absorb diffuse radiation because they are blocked by sunlit leaves, which are usually limited by low APAR (Chen et al., 1999; Mercado et al., 2009; Rap et al., 2018; Zhang et al., 2011). As a result, there are specific differences in APAR and LUE of the sunlit and shaded leaves, and the same treatment of sunlit and shaded leaves in big-leaf models will induce bias (Propastin et al., 2012; Wang et al., 2015). In fact, it has already been found that the MODIS GPP product underestimates GPP in regions with high vegetation coverage due to insufficient consideration of the contribution of shaded leaves (Chen et al., 2020; He et al., 2018; Zhang et al., 2012). In order to overcome this problem, a two-leaf LUE (TL-LUE) model was developed on the basis of the MOD17 model (He et al., 2013) by integrating the approach in the Boreal Ecosystem Productivity Simulator (BEPS) to separate the LAI and PAR of sunlit and shaded leaves (Chen et al., 1999; Liu et al., 1997). This TL-LUE model has been proved to outperform the big-leaf MOD17 model across a wide range of biomes, which highlights the necessity of separate treatments of sunlit and shaded leaves in LUE models (He et al., 2013; Zhou et al., 2016).

Nevertheless, the differences in LUE between different groups of leaves in the TL-LUE model are totally determined by the independent maximum LUE of sunlit and shaded leaves (ε_{msu} and ε_{msh}), which are the parameters manually set for different biomes (He et al., 2013; Zhou et al., 2016). The actual LUE of sunlit and shaded leaves are reduced from the optimum (ε_{msu} and ε_{msh}) by the same scalars of daily minimum temperature and vapor pressure deficit (VPD). However, the differences in LUE between sunlit and shaded leaves should mainly be attributed to the different intensity of radiation they received, and the maximum LUE is almost the same for the two groups of leaves (Chen et al., 1999; De Pury and Farquhar, 1997; Liu et al., 1997). The maximum LUE of a leaf is only decided by the physiological traits of the leaf itself, which should be nearly the same whether or not it is sunlit or shaded (Koyama and Kikuzawa, 2010; Leverenz, 1987). Although there are small differences in nitrogen content and carboxylation capacity between sunlit and shaded leaves because plants tend to allocate more resources to leaves at the top, which receive direct radiation more frequently than those at lower layers (Chen et al., 2012), the impacts of these differences on LUE would be much smaller than that of radiation (Hikosaka, 1996). So the similar physiological traits of sunlit and shaded leaves will certainly result in the similar maximum LUE, and the differences of LUE in them should be mostly caused by the different environmental conditions (Farquhar et al., 1980; Haxeltine and Prentice, 1996). Even though slight differences should exist between sunlit and shaded leaves in their temperature and humidity environments, the large difference in the light intensity between them is the dominant factor on their LUE (Leverenz, 1987). A light response curve generally shows a rapid increase in the leaf photosynthesis rate with increasing incident radiation when the

radiation intensity is low and a much slower increase when the radiation intensity is high, i.e., photosynthesis becomes saturated at a high radiation intensity (Ogren, 1993; Perkins et al., 2006; Zheng et al., 2017). Such a light response curve suggests that the LUE in shaded leaves should be higher than that in sunlit leaves, because of the lower APAR absorbed by shaded leaves. As a result, the existing TL-LUE model with two prescribed LUEs for sunlit and shaded leaves has the following issues: (1) it does not capture the influence of radiation intensity variations on LUE for both sunlit and shaded leaves, and (2) the LUEs of sunlit and shaded leaves are independent of each other, while in reality they are related and their difference depends on the incoming radiation intensity, canopy structure, and other variables.

From the theoretical point of view, it is therefore necessary to develop a system in which sunlit and shaded leaf LUEs are determined mechanistically and cohesively. In some ecosystem models, such as BEPS (Chen et al., 1999; Liu et al., 1997) and BIOME-BGC (Hunt Jr and Running, 1992), a radiation scalar is used to scale stomatal conductance from its optimum value to reality. Since stomatal conductance and LUE are highly related, we attempt to use this scalar to improve the TL-LUE model. The main purpose of this study is to develop a modified TL-LUE model (RTL-LUE) with consideration of the influence of radiation on LUE using this radiation scalar and to demonstrate the improvements of RTL-LUE over TL-LUE in simulating GPP of terrestrial ecosystems derived from eddy covariance (EC) data for 12 vegetation types across the globe.

2. Data and methods

2.1. Data

In this study, the FLUXNET2015 dataset is applied to the parameterization and validation of the RTL-LUE and TL-LUE models, including the records of GPP, incoming solar radiation, air temperature, and VPD. The FLUXNET2015 dataset (www.fluxdata.org) is the latest published flux observations from EC towers with a standard format, including the refined data from different regional networks for 212 sites worldwide (Pastorello et al., 2017; Pastorello et al., 2020). Similar to many previous studies, GPP partitioned by the DT method (termed "GPP_DT_VU-T_REF") is employed as the true GPP, which is partitioned from NEE using a hyperbolic light response curve (Reichstein et al., 2005). The sites with more than one year of valid half-hour observations during 2001−2015 are all selected, and there are in total 169 sites and 1191 site-years covering 12 vegetation types in the International Geosphere-Biosphere Program (IGBP) classification system. The number of sites and site-years for each vegetation type are listed in Table 1, and the detailed information and references for each site can be found in Table S1. The half-hourly data are used because they can support the comparison of diurnal GPP variations.

The Global LAnd Surface Satellite (GLASS) LAI product from 2001 to 2015 is used to drive the TL-LUE and RTL-LUE models, as the description of vegetation canopy structure and used to calculate APAR (Xiao et al., 2016). The dataset is provided at a spatial resolution of 1 km and temporal resolution of 8 days, which has been proved to have a satisfactory performance in GPP simulation (Xiao et al., 2017; Xie et al., 2019). Furthermore, the MODIS MOD15A2H LAI products with a spatial resolution of 500 m and temporal resolution of 8 days are also acquired to investigate the sensitivities of GPP performance to LAI inputs in the TL-LUE and RTL-LUE models (Myneni et al., 2015), by comparing the accuracy of GPP simulation from the two different LAI products. In order to reduce the impacts of the residual cloud contamination and eliminate the unrealistically short-term fluctuations, both the GLASS and MODIS LAI time series data were smoothed with the modified Whittaker trend filtering method (Chu et al., 2021).

Table 1
Number of EC sites and site years for different vegetation types in the IGBP classification system.

Vegetation type[a]	DBF	DNF	EBF	ENF	MF	GRA	CRO	CSH	OSH	WET	SAV	WSA
Number of Site	19	1	12	41	8	32	13	1	11	18	7	6
Number of Site-years	147	3	70	326	76	214	103	4	68	86	45	49

[a] DBF: deciduous broadleaf forest; DNF: deciduous needleleaf forest; ENF: evergreen needleleaf forest; EBF: evergreen broadleaf forest; MF: mixed forest; GRA: grass; CRO: crop; CSH: closed shrub; OSH: open shrub; WET: wetlands; SAV: savannas; WSA: woody savannas.

2.2. TL-LUE model

The TL-LUE model (He et al., 2013) stems from the MOD17 algorithm and improves the calculation of canopy APAR and GPP after separating the canopy into sunlit and shaded leaf groups according to the BEPS model (Chen et al., 1999). GPP of a plant canopy is calculated as follows:

$$GPP = (\varepsilon_{msu} \times APAR_{su} + \varepsilon_{msh} \times APAR_{sh}) \times f(VPD) \times g(T_a) \qquad (1)$$

where ε_{msu} and ε_{msh} are the maximum light use efficiency of sunlit and shaded leaves, respectively; $APAR_{su}$ and $APAR_{sh}$ are the incoming PAR absorbed by sunlit and shaded leaves and calculated as follows:

$$APAR_{su} = (1-\alpha) \times \left[\frac{PAR_{dir} \times \cos(\beta)}{\cos(\theta)} + \frac{PAR_{dif} - PAR_{dif,u}}{LAI} + C\right] \times LAI_{su} \qquad (2)$$

$$APAR_{sh} = (1-\alpha) \times \left[\frac{PAR_{dif} - PAR_{dif,u}}{LAI} + C\right] \times LAI_{sh} \qquad (3)$$

where α is the canopy albedo that obtained related to vegetation types (Table. S2); β is the mean leaf-sun angle and the value for a canopy with spherical leaf angle distribution is set as 60°; θ is the solar zenith angle; PAR_{dif}, PAR_{dir}, and $PAR_{dif,u}$ are the diffuse, direct components of incoming PAR, and the diffuse PAR under the canopy, respectively, which are empirically partitioned according to the clearness index (R) following Chen et al. (1999); C represents the multiple scattering of direct radiation; LAI_{su} and LAI_{sh} are the LAI of sunlit and shaded leaves, separated according to the canopy LAI, clumping index (Ω) and solar zenith angle according to Chen et al. (1999). The LAI_{su} can be computed as follow, and the LAI_{sh} is the residual of LAI minus LAI_{su}.

$$LAI_{su} = 2 \times \cos(\theta) \times \left(1 - exp\left(-0.5 \times \Omega \times \frac{LAI}{\cos(\theta)}\right)\right) \qquad (4)$$

In equation (1), $f(VPD)$ and $g(T_a)$ are the scalars of VPD and minimum temperature, which are the same as it in the MOD17 model (Running et al., 2004), calculated as follows:

$$f(VPD) = \begin{cases} 0 & VPD \geq VPD_{max} \\ \dfrac{VPD_{max} - VPD}{VPD_{max} - VPD_{min}} & VPD_{max} < VPD < VPD_{max} \\ 1 & VPD \leq VPD_{min} \end{cases} \qquad (5)$$

$$g(T_a) = \begin{cases} 1 & T_a \geq T_{max} \\ \dfrac{T_a - T_{min}}{T_{max} - T_{min}} & T_{min} < T_a < T_{max} \\ 0 & T_a \leq T_{min} \end{cases} \qquad (6)$$

where VPD is the daily average VPD at day-time and T_a is the daily minimum temperature, which can be both calculated from the half-hour data; VPD_{max}, VPD_{min}, T_{max}, and T_{min} are parameters specific to vegetation types (Table S2).

2.3. Description of the RTL-LUE model

Due to the fact that the nutrient and environmental conditions be-

tween sunlit and shaded leaves are very similar, the difference in LUE between these two groups of leaves should mainly attribute to the different light intensities. According to the BEPS and BIOME-BGC models, the scalar of photosynthetic photon flux density (PPFD) can be used to quantify the response of stomatal conductance to light intensity (Chen et al., 1999; Hunt Jr and Running, 1992; Liu et al., 1997). After considering the scalar of PPFD for the photosynthesis of sunlit and shaded leaves, a TL-LUE model with radiation constraint on LUE (RTL-LUE) is developed, and the calculation of GPP can be modified as follows:

$$GPP = \varepsilon_{max}^* \times (f(PPFD_{su}) \times APAR_{su} + f(PPFD_{sh}) \times APAR_{sh}) \times f(VPD)$$
$$\times f(T_a) \qquad (7)$$

where ε_{max}^* is the maximum LUE of all the leaves within the canopy; $APAR_{su}$, $APAR_{sh}$ $f(VPD)$ and $g(T_a)$ are calculated in the same way as them in TL-LUE and the MOD17 model; $f(PPFD_{su})$ and $f(PPFD_{sh})$ are the radiation scalars for sunlit and shaded leaves, respectively, which are calculated by the PPFD of the two groups of leaves, using the same reciprocal function as follows:

$$f(PPFD) = \frac{b}{a \times PPFD + b} \qquad (8)$$

where a and b are the coefficients in the relationship between light intensity and LUE. b is set as a constant with the value of 1 mol m^{-2} hh^{-1}, and only the parameter a is used to control the response of LUE to PPFD and needs to be parameterized depending on different vegetation types. $PPFD$ (mol m^{-2} hh^{-1}) for sunlit and shaded leaves can be obtained from the absorbed PAR (PAR_{su} or PAR_{sh}) multiplied by a constant PAR-energy ratio of 4.55 mol/MJ (Chen et al., 1999).

2.4. Model Parameterization and evaluation

2.4.1. Model Parameterization

Similar to previous studies, the parameters VPD_{max}, VPD_{min}, T_{max}, T_{min}, Ω and α are empirically set both in TL-LUE and RTL-LUE models according to previous studies (He et al., 2013; Zhou et al., 2016), as shown in Table S2. Two parameters need to be further optimized in both the RTL-LUE model (ε_{max} and a) and the TL-LUE model (ε_{msu} and ε_{msh}). These four parameters were all optimized using the randomly selected one-year data for each site (Table S1), and the mean values of the sites with the same vegetation type are obtained. The shuffled complex evolution-University of Arizona method was employed to implement the optimization (Duan et al., 1992; Zhou et al., 2016), which evaluates the model performance with the agreement index (d):

$$d = 1 - \frac{\sum\limits_{i=1}^{N} (P_i - O_i)^2}{\sum\limits_{i=1}^{N} \left(\left|P_i - \overline{O}\right| + \left|O_i - \overline{O}\right|\right)^2} \qquad (9)$$

where N is the total simulated experiment data point; P_i and O_i represent the predicted GPP from the TL-LUE or RTL-LUE models and observed EC GPP, respectively; and $\overline{O}$ and $\overline{P}$ are the mean values of observations and predictions for all experimental data points.

2.4.2. Model evaluation

The accuracies of the GPP simulations from the two models were assessed against half-hourly, composited 8-day, and composited yearly EC GPP. The diurnal and seasonal variations of GPP were qualitatively compared, and a simple ratio of EC GPP and model simulations were used to quantitatively assess the fluctuation of the difference between modeled and observed GPP. In addition, three indexes were used for accuracy evaluation, including the coefficient of determination (R^2), the root-mean-square error (RMSE), and the mean predictive error (bias):

$$R^2 = \left(\frac{\sum_{i=1}^{N}(P_i - \overline{O})(O_i - \overline{O})}{\sqrt{\sum_{i=1}^{N}(P_i - \overline{P})^2}\sqrt{\sum_{i=1}^{N}(O_i - \overline{O})^2}} \right)^2 \tag{10}$$

$$RMSE = \sqrt{\frac{\sum_{i=1}^{N}(P_i - O_i)^2}{N}} \tag{11}$$

$$bias = \frac{\sum_{i=1}^{N}(O_i - P_i)}{N} \tag{12}$$

3. Results

In this section, the parameterized maximum LUE in the TL-LUE and RTL-LUE models are compared, and the performances in GPP estimation from the two models are evaluated against the EC GPP. The results at half-hourly, 8-day, and yearly scales are all compared first, and then the diurnal and seasonal variations of GPP simulations from the two models are further evaluated.

3.1. Comparison of the parameterized maximum LUE

Two parameters need to be optimized both in two models, i.e., a and ε^*_{max} in RTL-LUE and ε_{msu} and ε_{msh} in TL-LUE. The mean values, standard deviations (SD), and CV of them in different vegetation types are compared in Table 2. Overall, the values of ε^*_{max} in the RTL-LUE model are lower than ε_{msh} and higher than ε_{msu} in the TL-LUE model among all the 12 vegetation types. In the TL-LUE model, the value of ε_{msh} is much higher than ε_{msu} because shaded leaves only have the chance to absorb the diffuse radiation, with PAR_{sh} always much lower than PAR_{su} and usually lies between the light compensation point and the light saturation point. According to the light response curve, the photosynthetic rate will decrease with increasing APAR, so the LUE of shaded leaves should

be higher than that of sunlit leaves. Furthermore, the mean values of ε_{msh} and ε_{msu} are also compared with ε^*_{max}, which shows a very similar variation among different vegetation types with an R^2=0.73. The mean values of ε_{msh} and ε_{msu} are generally lower than ε^*_{max}, which may be due to the reason that shaded leaves are always more than sunlit leaves in a canopy. Since the value of ε_{msh} is generally higher than that of ε_{msu}, the arithmetic mean of ε_{msh} and ε_{msu} with the same weight should be lower than the actual maximum LUE, in which the shaded leaves have a higher weight than sunlit leaves. So the variation of ε^*_{max} among different vegetation types is also more similar to that of ε_{msh} with R^2=0.79, but R^2 is only 0.34 for ε_{msu}.

The ranks of ε_{msh} and ε_{msu} among different vegetation types are consistent with the results of Zhou et al. (2016), in which the highest values are found in crops and the lowest values are in savannas. In this study, because three more vegetation types are included, ε_{msu} and ε_{msh} of crops are both the second-highest, and the ε_{msh} in savannas are also the second-lowest and only slightly higher than those of DNF. For ε^*_{max}, the highest value is also found in crops, and the lowest value is in closed shrubs. There are some differences between the mean values of ε_{msu} and ε_{msh} in this study and Zhou et al. (2016) for overlapping nine vegetation types. The main reason is that there are many more sites employed to optimize the parameters in this study, in order to verify the reliability of the model across as many sites as possible. Zhou et al. (2016) parameterized the TL-LUE model by carefully excluding the flux sites with heterogeneous vegetation types. The accuracy of GPP simulations based on the suggested parameters for the nine vegetation types in Zhou et al. (2016) is also evaluated, and the results are very similar to those in this study, with a difference generally lower than 0.01 in R^2, as shown in Table S3. Because there are three more vegetation types used in this study, we do not apply the parameters suggested in Zhou et al. (2016) but optimize them ourselves for a fair comparison with the improved RTL-LUE model.

The parameter of a also shows significant differences among different vegetation types. The highest a values are found in the EBF and crops, and the lowest values are in SAV and WSA. Due to the reciprocal scalar of PPFD used in this study, the larger the value of a for a vegetation type, the more sensitive to PAR the vegetation type is (Chen et al., 1999).

3.2. Validation of the GPP simulations

3.2.1. Half-hourly results

In this study, GPP was estimated based on the half-hourly EC observation datasets, and the accuracy of simulated results was first evaluated at the half-hour scale, and further assessed after they were

Table 2

Mean value, Standard Deviations (SD), and CV of the optimized parameter of a and different maximum LUE, i.e. ε^*_{max}, ε_{msu}, and ε_{msh}, for different vegetation types.

Vegetation type [a]	Mean (g C MJ^{-1}) [b]				SD (g C MJ^{-1}) [b]				CV [c] (%)			
	a	ε^*_{max}	ε_{msu}	ε_{msh}	a	ε^*_{max}	ε_{msu}	ε_{msh}	a	ε^*_{max}	ε_{msu}	ε_{msh}
DBF	1.54	2.85	0.78	3.13	1.08	0.91	0.31	0.87	69.90	32.08	39.59	27.82
DNF	0.69	1.68	0.70	1.89	/	/	/	/	/	/	/	/
EBF	1.02	2.16	0.72	2.40	0.76	0.83	0.12	0.60	74.37	38.46	16.65	25.06
ENF	0.79	2.14	0.88	2.57	0.51	0.58	0.32	0.74	64.79	27.07	36.99	28.91
MF	0.81	2.54	1.23	2.86	0.40	0.76	1.17	0.61	49.35	30.05	95.37	21.52
GRA	0.63	2.39	1.07	3.02	0.53	1.39	0.54	1.89	84.12	58.01	50.59	62.47
CRO	1.43	3.32	1.25	3.22	1.77	2.04	0.57	1.59	123.58	61.33	46.05	49.45
CSH	0.59	1.68	0.70	2.10	/	/	/	/	/	/	/	/
OSH	0.57	1.58	0.68	2.35	0.61	1.01	0.40	1.83	106.43	63.97	58.60	77.80
WET	1.36	2.82	1.14	3.26	2.18	1.85	0.66	2.36	159.96	67.08	57.63	72.49
SAV	0.20	1.60	1.41	1.91	0.00	1.10	0.98	1.16	0.00	66.85	69.57	60.93
WSA	0.46	1.96	0.97	3.01	0.31	0.70	0.27	1.57	68.14	31.95	28.27	52.01

[a] The abbreviations of different vegetation types are the same as it in Table 1

[b] the unit is only for ε^*_{max}, ε_{msu}, and ε_{msh}, and the $PPFD_a$ is a parameter without unit

[c] CV=100% × SD/Mean.

Figure 1. Comparison of the accuracy of GPP simulations against tower measurements (EC GPP) for the original TL-LUE model and the RTL-LUE model at 169 EC observation sites: (a) R2, (b) RMSE.

composited into the 8-day and yearly GPP in the following two sections. As shown in Fig. 1, R^2 and RMSE for GPP simulations from the TL-LUE and RTL-LUE models were calculated at 169 EC sites against the EC GPP, and compared in a scatterplot. It can be observed that the RTL-LUE model outperforms the TL-LUE model at almost all sites, with a higher R^2 and lower RMSE. There are in total 160 out of 169 sites showing a reduced RMSE after considering the radiation scalar in the RTL-LUE model, and the number is 144 for sites with a higher R^2. The largest improvement in R^2 is 0.097, and the largest reduction in RMSE is 0.15 g C m^{-2} hh^{-1}. There are 102 sites showing an improvement in R^2 more than 0.02, and 111 sites showing a reduction in RMSE more than 0.02 g C m^{-2} hh^{-1}. The improvements in R^2 are even larger and more stable at the sites with higher R^2 values, as shown in Fig. 1 (a). For example, there are in total 56 sites with R^2 greater than 0.7, and 54 out of them show an improved R^2 with a mean increase of 0.04. On the contrary, the reductions in RMSE are more remarkable at the sites with higher RMSE, as shown in Fig. 3 (b). Among the 70 sites with RMSE higher than 0.15, 69 of them show a lower RMSE in the RTL-LUE model with a mean reduction of 0.068 g C m^{-2} hh^{-1}.

The three indexes of GPP simulations from the TL-LUE and RTL-LUE models were also compared among the 12 different vegetation types, by calculating the mean value for all sites with the same vegetation type. As shown in Table. 3, although the GPP simulated by the TL-LUE model agrees well with the EC data, the RTL-LUE model further improves the simulation of GPP in all of the 12 vegetation types. Overall, the TL-LUE model shows mean values of 0.58 and 0.14 g C m^{-2} hh^{-1} for R^2 and

RMSE, respectively, and the corresponding values are 0.61 and 0.10 g C m^{-2} hh^{-1} for the RTL-LUE model with an improvement in R^2 by 0.03 and a reduction in RMSE by 0.04 g C m^{-2} hh^{-1}. The rank of vegetation types based on the value of R^2, RMSE, or bias are all the same. The value of R^2 ranges from 0.38 for open shrubs to 0.78 for closed shrubs in the results of the TL-LUE model, and the range is from 0.40 to 0.82 for the RTL-LUE model. The RTL-LUE model consistently performs much better in the five types of forest sites, and a considerable improvement is found in the deciduous broadleaf forest sites, with a difference of 0.06, 0.09 g C m^{-2} hh^{-1}, and 0.06 g C m^{-2} hh^{-1} for R^2, RMSE, and bias, respectively. However, almost no improvements can be observed at the sites covered by savannas, only with a limited reduction in RMSE and bias of about 0.01 g C m^{-2} hh^{-1}.

3.2.2. 8-day results

In order to further evaluate the accuracy of GPP simulated by the TL-LUE and RTL-LUE models, the half-hourly data were composited using the 8-day sum to match the time interval of LAI data. The density scatterplot of all the data points for the 12 individual vegetation types are provided in Fig. 3 (TL-LUE) and Fig. 4 (RTL-LUE), respectively. It can be observed that the overall accuracies of both the two models are improved after the 8-day composition, with a mean R^2 of 0.64 and 0.65 for the GPP simulations from the TL-LUE and RTL-LUE models, and the RMSE is 19.01 g C m^{-2} 8d^{-1} and 13.91 g C m^{-2} 8d^{-1}, respectively. The R^2 of grass, woody savannas, and open shrubs sites even show an improvement in R^2 greater than 0.18. However, the accuracies of GPP

Table 3
Statistic of the GPP simulation accuracy for different vegetation types.

Vegetation type [a]	TL-LUE			RTL-LUE			Difference [b]		
	R^2	RMSE [c]	bias [c]	R^2	RMSE [c]	bias [c]	R^2	RMSE [c]	bias [c]
DBF	0.68	0.20	0.11	0.74	0.12	0.04	0.06	-0.09	-0.06
DNF	0.65	0.06	0.02	0.67	0.05	0.02	0.02	-0.01	-0.01
EBF	0.66	0.17	0.07	0.69	0.11	0.02	0.03	-0.07	-0.05
ENF	0.66	0.12	0.03	0.68	0.09	0.00	0.02	-0.04	-0.03
MF	0.71	0.21	0.05	0.73	0.15	0.01	0.02	-0.06	-0.04
GRA	0.51	0.12	0.04	0.53	0.10	0.02	0.02	-0.03	-0.02
CRO	0.41	0.18	0.06	0.43	0.15	0.03	0.02	-0.03	-0.03
CSH	0.78	0.13	0.08	0.82	0.07	0.01	0.04	-0.07	-0.07
OSH	0.38	0.06	0.02	0.40	0.04	0.01	0.02	-0.01	-0.01
WET	0.59	0.14	0.07	0.62	0.09	0.03	0.03	-0.05	-0.04
SAV	0.49	0.12	0.02	0.49	0.11	0.01	0.00	-0.01	-0.01
WSA	0.53	0.12	0.07	0.54	0.09	0.03	0.01	-0.04	-0.04
All	0.58	0.14	0.05	0.61	0.10	0.02	0.03	-0.04	-0.03

[a] The abbreviation of different vegetation types are the same as it in Table 1
[b] Difference means the R^2, RMSE, and bias of RTL-LUE model minus the corresponding value of TL-LUE model
[c] the units of RMSE and bias are g C m^{-2} hh^{-1}.

simulations in some vegetation types decrease compared to the half-hourly data, and typically the closed shrubs sites show a decline in R^2 by −0.19. For the 8-day data, the most significant improvement of the RTL-LUE model over the TL-LUE model is found at open shrub sites with an increase of 0.03 for R^2 and a decrease of 1.95 g C m^{-2} 8d^{-1} for RMSE. The best accuracy can be found in the deciduous broadleaf forest sites with an R^2 of 0.77 and 0.80 for the TL-LUE and RTL-LUE models, respectively. The worst performance is found at crop sites with an R^2 of 0.34 and 0.36 for the two models, respectively. GPP of crops are not well simulated in both two models, with an overestimation in low EC GPP points and underestimation in high EC GPP points. Similar simulation results for crops were reported in previous studies using the BEPS model and the MOD17 model, and failure to account for the impacts on irrigation and fertilization in crops was considered to be the main reason for the low performance of these models (Zhang et al., 2012).

3.2.3. Yearly results

In order to conduct an overall assessment of GPP simulated by the TL-LUE and RTL-LUE models, half-hourly data were further summed into yearly data. The density scatterplots of simulated GPP against the EC GPP of all site-years are shown in Fig. 4. Although GPP simulated by the TL-LUE model already shows good agreement with EC GPP, the results from the RTL-LUE model further confirm its superiority, with improvements of R^2 (+0.02), RMSE (−165.28 g C m^{-2} year^{-1}), and bias (−202.59 g C m^{-2} year^{-1}). Furthermore, it can be observed that the TL-LUE model tends to overestimate GPP, especially in the points with high GPP values. This phenomenon is consistent in Fig. 2. However, this problem is relieved by the RTL-LUE model after considering the radiation scalar, which could suppress the high value of GPP when radiation was high.

In general, from the analysis above, it can be summarized that the RTL-LUE model can improve the accuracy in GPP simulation after using the radiation scalar, at half-hourly, 8-day, and yearly time scales. For all or individual vegetation types, the GPP simulated by the RTL-LUE model shows increased R^2 and reduced RMSE and bias relative to the TL-LUE model in comparison with EC observations.
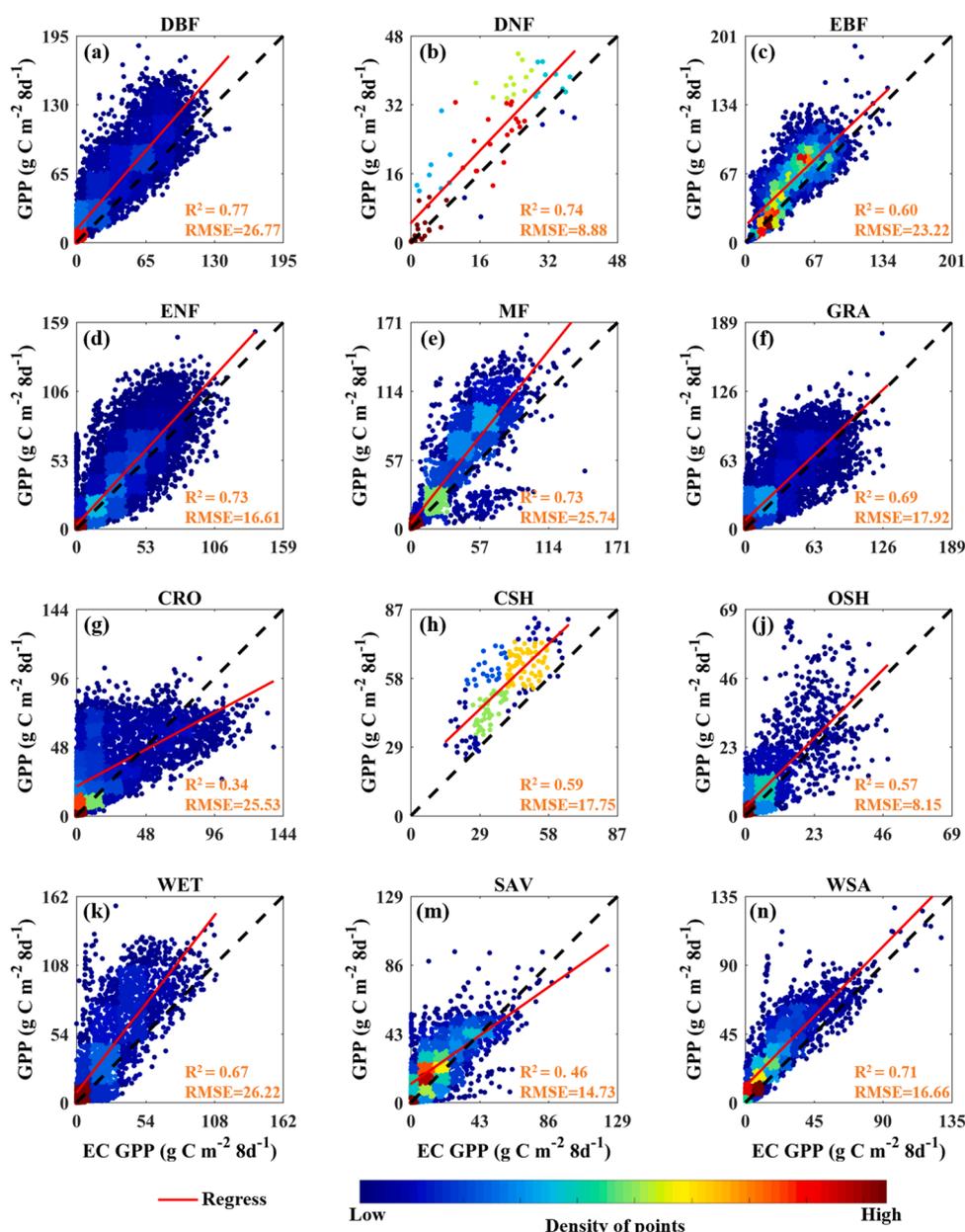
Figure 2. Validation of GPP simulations from the TL-LUE model after composited into 8-day totals.

3.3. Diurnal variation of GPP

Since GPP was calculated based on the half-hourly dataset, the diurnal variation of GPP simulated by the TL-LUE and RTL-LUE models can be compared against EC data. In order to validate the diurnal variation of GPP, the Coefficients of Variation (CV) of the Ratio (R_CV) between EC GPP and simulated GPP (Ratio=EC GPP/simulated GPP) in each site-days were calculated. Since the Ratio represents the relative difference between the simulated GPP and EC GPP, the R_CV, which denotes the variation of Ratio in each day, can certainly assess the consistency of the diurnal variation between EC GPP and GPP simulations. If the diurnal variation of simulated GPP is entirely the same as the EC GPP, the R_CV should be zero. As a result, the smaller the R_CV, the better the diurnal variation of the simulated GPP is. In addition, the R^2 and RMSE between the simulated GPP and EC GPP in all the 333,919 site-days were also calculated, and the mean values of them for 12 vegetation types are displayed in Table. 4. It can be observed that the mean R_CV of GPP simulations from the RTL-LUE model is obviously lower than that from the TL-LUE model, either in all or individual vegetation types. Among all the 333,919 site-days, 92.9% of them show a lower R_CV in the GPP simulations from the RTL-LUE model compared to the TL-LUE model simulations, while the ratio is 83.4% and 76.5% for a higher R^2 and lower RMSE. The overall improvement of R_CV reaches 11.5%, which is almost one-third of the R_CV for the GPP estimations from the TL-LUE model. The most remarkable improvement can be found at the sites covered by evergreen broadleaf forest and open shrubs, with differences greater than 0.14 in R-CV and 0.04 in R^2. The diurnal variation of GPP at savannas sites is similar between the two models, with almost the same R^2 and very small differences in RMSE and R_CV.

The diurnal variation of GPP estimations was further qualitatively compared against the EC observations, by plotting representative diurnal variation curves from 12 different months and 12 different vegetation types. As shown in Fig. 5, monthly mean values for each half-hour were calculated and plotted. The monthly means were used in order to minimize the fluctuations in a single day and to enhance the dependability of the comparisons. For all the months and vegetation types, both the GPP simulations from the two models and EC GPP consistently reach the peak at noon with the highest radiation. However, in almost all the 12 plots, the TL-LUE model tends to overestimate GPP at the peak, while the GPP simulated by the RTL-LUE model agrees well with EC GPP in this condition. The improvement in simulating the peak GPP values with the RTL-LUE model can mainly attribute to the use of

the radiation scalar in the model. Because no radiation scalar is used in the TL-LEU model, the LUEs of both sunlit and shaded leaves do not vary with radiation, causing underestimation of GPP at low PAR but overestimation at high PAR, even though the LUEs are optimized using the observed GPP to capture their mean values. The use of the radiation scalar avoids this issue, and this is the main improvement of RTL-LUE over TL-LUE. While in the morning and dusk, when the radiation scalar does not play an important role because radiation is generally low, both the GPP simulated by TL-LUE and RTL-LUE models agree well with the EC GPP. For the sites covered by the savannas, the diurnal variation of GPP simulated by the two models are almost the same, which is mostly due to the low value of a used (0.20, the lowest among 12 vegetation types), so the variation of GPP will not be sensitive to the intensity of radiation.

3.4. Seasonal variation of GPP

The seasonal variation is also critical when evaluating the reliability of GPP simulations. Similar to the assessment of diurnal variation, the composited 8-day data were employed to calculate R^2, RMSE, and R_CV between the simulated GPP and EC data for all site-years. The 8-day data were used to eliminate the diurnal variation and only assess the seasonal variation. The mean values of the three indexes for 12 vegetation types are summarized in Table 5. There are some differences between the results in Section 3.1.2, where the indexes are calculated for each site, but the evaluation here is made for individual site-years. The conclusions are consistent with those for the diurnal variation. The seasonal variation of GPP simulated by the RTL-LUE model agrees better with EC GPP than that by the TL-LUE model, either in all or individual vegetation types. Overall, about 92.3% of the 1191 site-years show a declined R_CV for the GPP simulations from the RTL-LUE model comparing to the TL-LUE model results, and the ratio is 87.5% and 81.3% for a higher R^2 and lower RMSE for RTL-LUE. The quantitative improvements in seasonal variation are not as significant as those in the diurnal variation. The most considerable decrease in R_CV is 4.5% in ENF, and the greatest improvement in R^2 is 0.02 and the greatest reduction in RMSE is 9.86 g C m^{-2} 8d^{-1} in DNF and CSH. Although RMSE and R_CV decrease in all 12 vegetation types when TL-LUE is replaced with RTL-LUE, R^2 is almost the same for SAV, CSH, and ENF.

The seasonal variation curves of some representative site years for the 12 vegetation types were also selected for qualitative assessment, as displayed in Fig. 6. The seasonal variations of GPP simulated by both models show very similar seasonal variation with EC GPP in almost all

Table 4

Statistics of the diurnal variation consistency between half-hourly GPP simulations and EC GPP over all site-days.

Vegetation types [a]	TL-LUE			RTL-LUE			Percentage [b] (%)		
	R^2	RMSE[c]	R_CV[d] (%)	R^2	RMSE[c]	R_CV[d] (%)	R^2	RMSE[c]	R_CV[d]
DBF	0.91	0.16	33.24	0.95	0.09	17.83	83.95	78.17	90.75
DNF	0.91	0.05	33.58	0.93	0.04	22.67	68.78	80.41	89.18
EBF	0.92	0.14	31.69	0.96	0.09	18.27	93.81	80.73	97.63
ENF	0.91	0.09	32.44	0.95	0.06	21.53	94.58	62.93	97.41
MF	0.90	0.16	29.00	0.91	0.11	20.00	91.31	79.44	94.15
GRA	0.85	0.09	39.37	0.88	0.07	28.57	81.29	71.28	91.35
CRO	0.90	0.12	33.02	0.94	0.10	19.17	84.88	68.25	91.54
CSH	0.94	0.12	26.08	0.95	0.06	22.45	95.75	86.28	99.38
OSH	0.77	0.04	53.32	0.82	0.03	39.16	84.10	74.59	95.04
WET	0.92	0.11	29.73	0.95	0.07	18.63	84.17	77.17	91.30
SAV	0.78	0.09	41.36	0.78	0.08	40.51	50.78	73.95	79.83
WSA	0.79	0.10	41.52	0.79	0.07	31.59	58.23	84.06	87.36
All	0.88	0.10	35.40	0.91	0.07	23.95	83.55	76.49	92.09

[a] The abbreviation of different vegetation types are the same as it in Table 1

[b] Percentage means the percentage of site-days that the diurnal variation of GPP simulated by RTL-LUE model was better than TL-LUE model, i.e., with a higher R^2, lower RMSE, and lower R_CV

[c] unit of RMSE is g C m^{-2} hh^{-1}

[d] R_CV means the Coefficients of Variation (CV) of the ratio (EC GPP/simulated GPP), and represents the diurnal fluctuation of the difference between GPP simulations and EC observations.

Table 5
Statistics of the seasonal variation consistency between 8-day GPP simulations and EC GPP over all site-years.

Vegetation type [a]	TL-LUE			RTL-LUE			Percentage [b] (%)		
	R^2	RMSE [c]	R_CV [d] (%)	R^2	RMSE [c]	R_CV [d] (%)	R^2	RMSE [c]	R_CV [d]
DBF	0.83	24.66	52.80	0.84	15.67	50.00	95.68	87.05	81.29
DNF	0.83	8.34	44.94	0.85	7.16	41.69	100.00	100.00	100.00
EBF	0.48	22.02	37.47	0.49	15.28	31.91	66.67	91.30	98.55
ENF	0.84	14.41	54.83	0.84	11.28	49.81	64.09	69.97	99.07
MF	0.90	24.48	46.02	0.91	16.71	40.95	87.32	95.77	95.77
GRA	0.64	14.68	62.65	0.65	12.57	58.92	76.53	75.59	94.37
CRO	0.41	24.68	74.77	0.42	21.97	72.01	90.29	90.29	92.23
CSH	0.63	17.69	25.67	0.63	7.83	24.90	75.00	75.00	75.00
OSH	0.53	6.94	73.82	0.54	5.64	68.99	69.12	79.41	97.06
WET	0.82	20.47	57.10	0.83	14.16	54.53	80.49	71.95	81.71
SAV	0.63	13.05	48.07	0.63	12.71	47.48	61.36	93.18	79.55
WSA	0.57	14.56	48.72	0.58	10.08	44.20	83.67	95.92	93.88
All	0.71	17.59	52.24	0.72	13.40	48.78	81.27	87.54	92.79

[a] The abbreviation of different vegetation types are the same as it in Table 1
[b] Percentage means the percentage of site-days that the diurnal variation of GPP simulated by RTL-LUE model was better than TL-LUE model, i.e., with a higher R^2, lower RMSE, and lower R_CV
[c] unit of RMSE is g C m^{-2} 8d^{-1}
[d] R_CV means the CV of the ratio (EC GPP/simulated GPP), and represents the seasonal fluctuation of the difference between GPP simulations and EC observations.

vegetation types, except for crops. The apparent decline of EC GPP during the DOY (day of the year) from 193 to 257, which may be caused by crop harvest, cannot be well simulated by both models. It may be mostly caused by the uncertainties in LAI data, which cannot sufficiently capture crop growth stages. The unsatisfactory results for the evaluation of crops in Section 3.2.2 may also be caused by the same reason, as the low values in EC GPP during the harvest period are all overestimated in Fig. 2 and 3 (g). Furthermore, the overestimation of GPP by the TL-LUE model can also be found in the growing season, such as the vegetation types of DBF, EBF, ENF GRA, and CSH. The seasonal variation of GPP simulated by the two models is almost the same for the DNF and SAV sites, and both of them agreed well with the EC GPP.

In general, the TL-LUE GPP initially agrees well with the EC observations in most vegetation types, but the RTL-LUE model can further improve the consistency with observations. Although the seasonal variations of GPP simulated by the RTL-LUE model are better than those by the TL-LUE model in most site years, the improvements are not as significant as it in the diurnal variation, either in the quantitative and qualitative analysis.

4. Discussion

In this section, the relationship between PAR and canopy LUE is firstly discussed to exam the reasonability of the radiation scalar used in the RTL-LUE model. Afterward, the sensitivity of GPP estimation and canopy LUE to PAR variation is analyzed, and the reason for the overestimation of GPP in the TL-LUE model is further explored. Finally, the sensitivity of GPP simulation to remote sensing LAI inputs is investigated, and the improvements and limitations of the RTL-LUE model are summarized.

4.1. Relationship between PAR and canopy LUE in site observations

In order to the exam reasonability of adopting the scalar of radiation in the GPP simulation, it is necessary to verify the relationship between LUE and PAR based on the site observations. Since there are no LUE measurements at the EC sites, the canopy LUE was approximated by the ratio of the observed GPP and PAR (LUEc=GPP/PAR) (He et al., 2013). LAI or APAR was not employed here to avoid errors induced by remote sensing data, so the analysis based on measurements only can capture the true relationship between LUE and PAR. As shown in Fig. 7, the density scatterplot of LUEc and PAR at specific sites among 12 vegetation types are demonstrated, and the linear and reciprocal fitting lines are also included. The LUEc decreases with the increase in PAR in all

vegetation types. However, the decrease is not linear, with the rate of decrease higher at the lower PAR values and gradually becoming slower with increasing PAR. As a result, it can be concluded that the reciprocal function can better fit the relationship between LUEc and PAR, and is suitable to represent the scalar of radiation on GPP estimation.

Furthermore, the quantitative assessments were also conducted by calculating the mean values of R^2 and RMSE for the linear and reciprocal regressions for the 12 vegetation types. The index of bias was excluded because it is too small to compare. As listed in Table 6, the reciprocal function can fit the relationship between LUEc and PAR much better than the linear regression, with higher R^2 and lower RMSE. Overall, the reciprocal function outperforms the linear relationship in 98.8% of the 169 sites. Only two sites covered by EDF and GRA (site names are AU-Ync and FR-Fon) show an R^2 lower than 0.05 for both two functions. The improvements of R^2 range from 0.01 in crops to 0.07 in EBF. Both methods perform the worst in crops, only with an R^2 lower than 0.1 and very high RMSE around 0.34 g C MJ^{-2}. It may also be the reason for the unsatisfactory result in GPP simulations by both TL-LUE and RTL-LUE models. Even in this condition, the reciprocal regression is better than the linear regression at all crop sites. In general, it can be concluded that the canopy LUE (approximated by LUEc=GPP/PAR) shows a reciprocal relationship with PAR, so it is reasonable to use the radiation scalar in the RTL-LUE model.

4.2. Sensitivity of GPP Simulations to PAR

The comparison of GPP simulations with EC measurements indicates that the TL-LUE model tends to overestimate GPP under the conditions of high incoming radiation. In order to further investigate the degree of overestimation, the difference of GPP simulations and EC GPP (ΔGPP = GPP$_{simulation}$ − GPP$_{EC}$) are binned according to the magnitude of incoming PAR. As shown in Fig. 8, both models tend to underestimate GPP in the conditions of very low PAR, and gradually overestimate GPP at high PAR values. GPP simulations from the two models can agree well with the EC GPP with little differences in the low incoming PAR range. While, with the increase in PAR, the overestimation of the TL-LUE model generally becomes more and more severe and reaches a very high level. In contrast, although the overestimation of the RTL-LUE model can also be observed in some vegetation types, the magnitude of overestimation is much smaller and becomes stable even the PAR is very high. The RTL-LUE model dramatically alleviates the sensitivity of simulated GPP to PAR, by suppressing the high GPP to be more close to the EC measurements in the conditions of high incoming PAR. The difference between the two models at SAV sites is still very small, which is consistent with
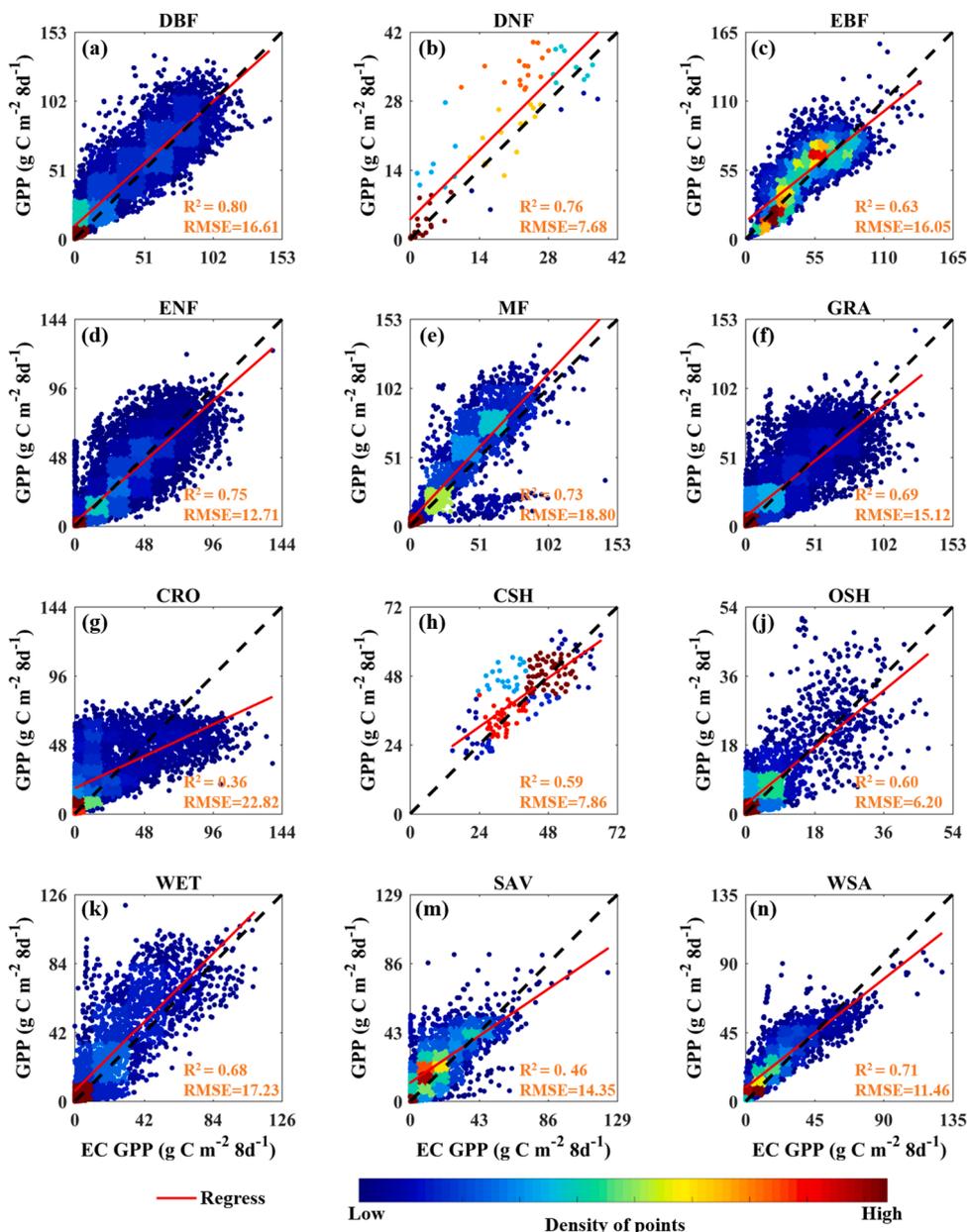
Figure 3. Validation of GPP simulations from the RTL-LUE model after composited into 8-day totals.
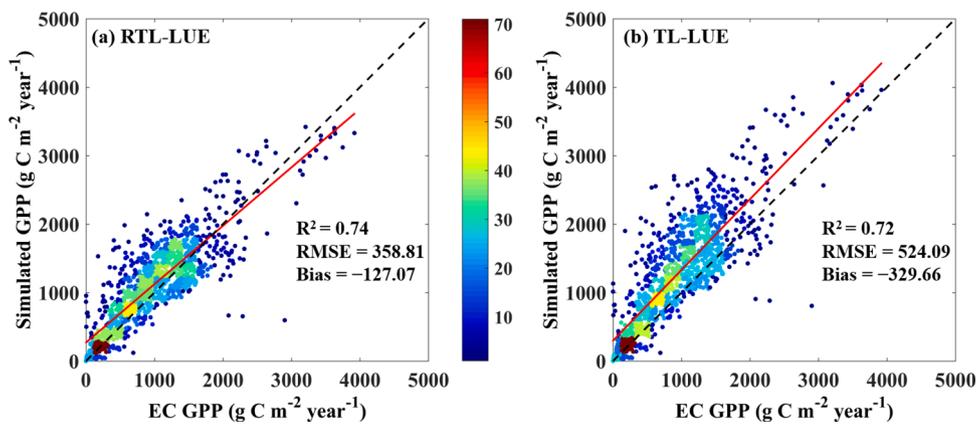
Figure 4. The relation between the yearly EC GPP and the simulated results from (a) the RTL-LUE model and (b) the TL-LUE model.
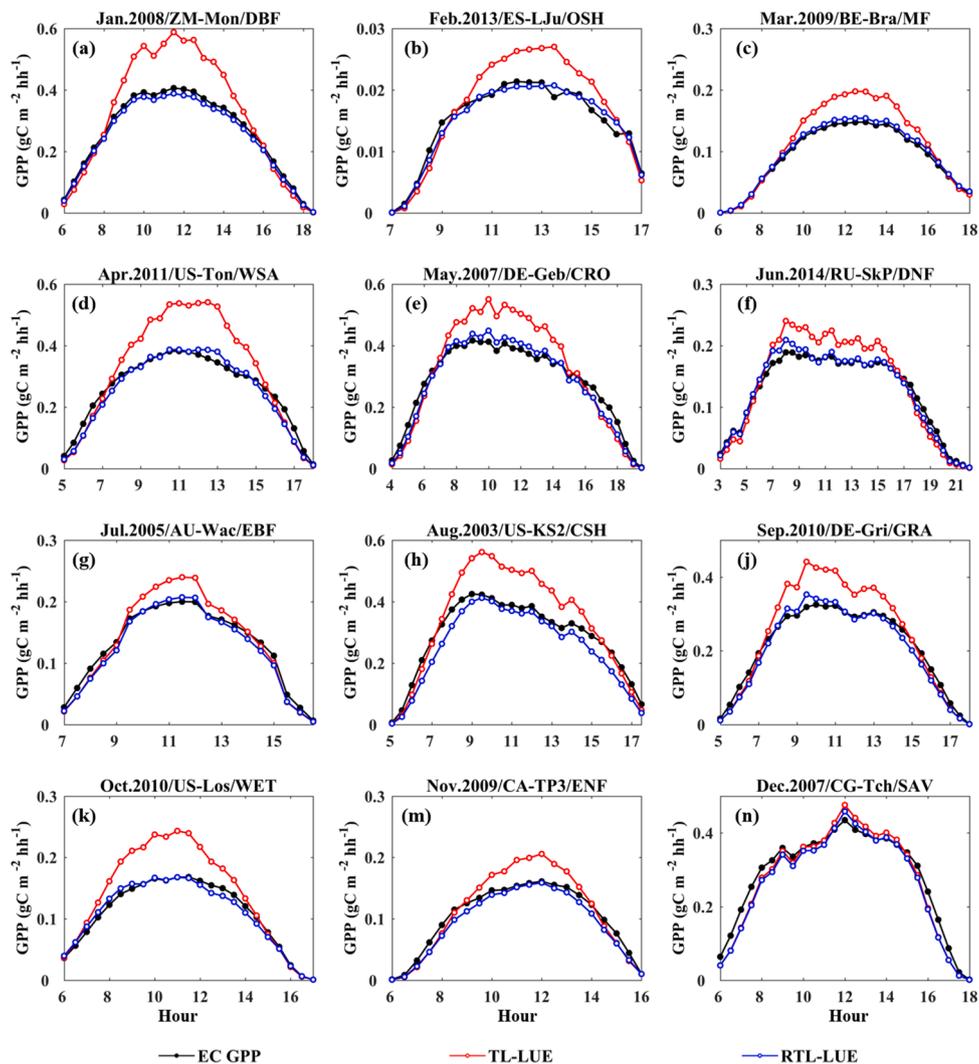
Figure 5. Diurnal variation of EC GPP and GPP simulated by the TL-LUE and RTL-LUE models in different months and different vegetation types. The title of each subplot is named as "month. year/site name/vegetation types".

the results above due to the small value of *a*.

The main reason for the overestimation of GPP by the TL-LUE model in conditions of high incoming PAR is the use of constant LUE values without scaling for radiation. The percentage of point numbers within different PAR ranges is also calculated and displayed as the black triangular line in Fig. 8. Obviously, much more points are concentrated in the area with low incoming PAR, where the GPP simulated by the TL-LUE model agrees well with the EC GPP. As a result, the parameter optimization tends to obtain a relatively high value of ε_{msu} and ε_{msh} that suit for the majority conditions of low incoming PAR, in order to ensure the overall accuracy. Besides, because only the scalars of VPD and temperature are considered in the TL-LUE model, the LUEs of sunlit and shaded leaves will not directly change with PAR. So the constantly high ε_{msu} and ε_{msh} will certainly induce the unreasonable high LUE, resulting in the overestimation of GPP in the conditions of high incoming PAR. This problem can be significantly alleviated in the RTL-LUE model, because the scalar of incoming PAR is used to suppress the LUE at higher incoming PAR.

The canopy LUEs (LUEc=GPP/PAR) calculated by GPP simulations and EC observations are also averaged over 0.01 bins of incoming PAR (MJ m^{-2} hh^{-1}), as shown in Fig. 9. At all sites, the EC observed LUEc significantly decreases with PAR, and the RTL-LUE model can generally reproduce these trends. However, the variation of LUEc simulated by the TL-LUE model shows more flat trends. Obviously higher LUEc values in

the TL-LUE model can be observed at high incoming PAR, indicating that the maximum LUE could not be reduced to the actual LUE only by the scalars of VPD and temperature in the TL-LUE model, and thus leading to the overestimation of GPP at high incoming PAR. It is reasonable to consider the constraint of radiation in the RTL-LUE model, and the overestimation could be significantly alleviated by *f(PPFD)*.

4.3. Improvements and limitations

In this study, an RTL-LUE model is developed to improve GPP simulation by considering the scalar of radiation on vegetation LUE, based on the concept that LUE should decrease with increasing incoming PAR (Chen et al., 1999; Koyama and Kikuzawa, 2010; Sinclair and Horie, 1989). The model is modified based on a TL-LUE model by giving the same maximum LUE to the sunlit and shaded leaves, rather than prescribing two different maximum LUE values for these two leaf groups. Generally, the maximum LUE, which is controlled by physiological traits of leaves in a plant canopy, should be almost the same for shaded or sunlit leaves (Leverenz, 1987). Although limited differences may exist in the distributions of nutrients and leaf age between sunlit and shaded leaves, their impacts on the maximum LUE are expected to be small (Hikosaka, 1996). The major differences between sunlit and shaded leaves are the environmental conditions, i.e., radiation, temperature, and humidity, which will only impact the actual LUE rather
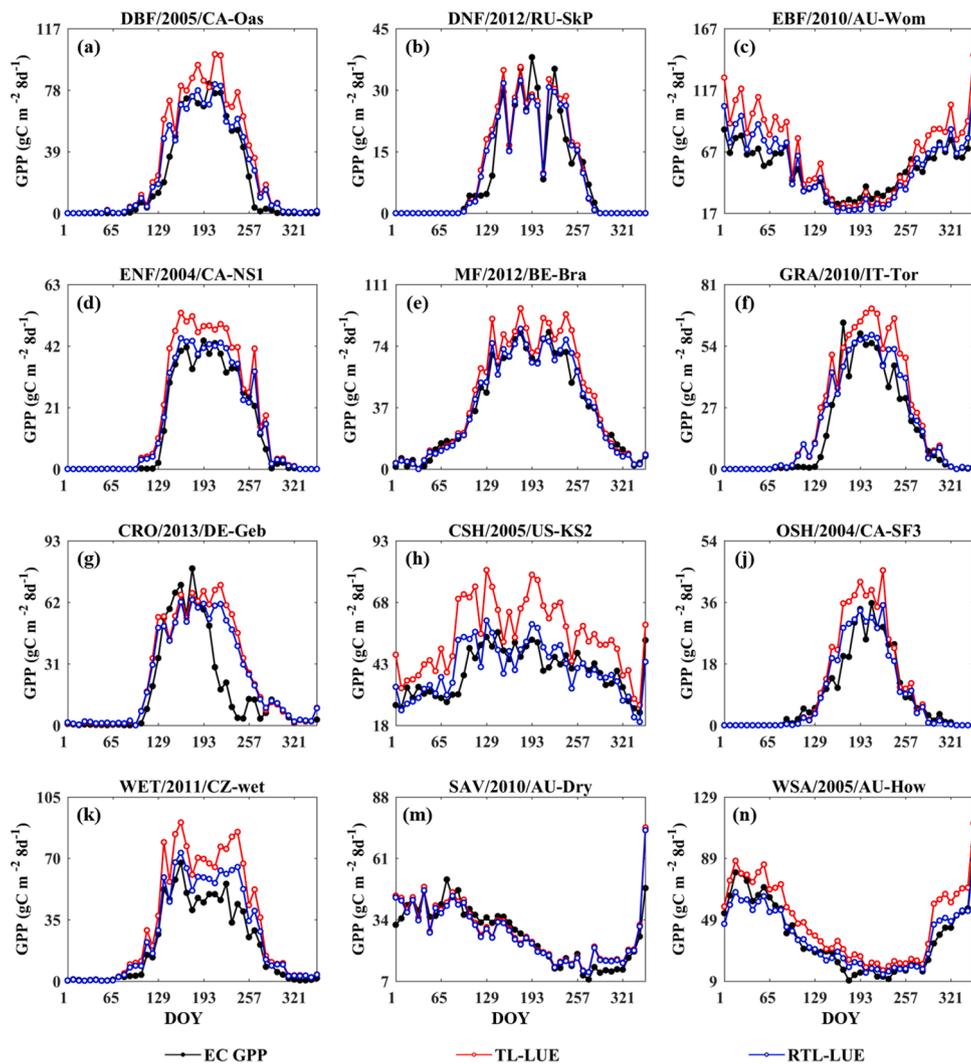
Figure 6. Seasonal variations of EC GPP and GPP simulated by the TL-LUE and RTL-LUE models for different vegetation types. The title of each subplot is named as "vegetation types/site year/site name", DOY means the day of the year.

than maximum LUE. Among these environmental variables, radiation is the primary factor because the radiation absorbed by shaded leaves is undoubtedly much less than that by sunlit leaves (McCallum et al., 2013; Perkins et al., 2006). The results and analysis above have shown the effectiveness of the scalar of radiation in constraining the maximum LUE and representing the differences in LUE between sunlit and shaded leaves. After modifying the model, no additional data inputs are needed, and the number of parameters needed to optimize is also the same, which are ε_{msu} and ε_{msh} for the TL-LUE model and a and ε^*_{max} for the RTL-LUE model. If we take a as the fixed-parameter for environmental scalars, similar to VPD_{max}, VPD_{min}, T_{max}, or T_{min}, only ε^*_{max} is needed to optimize in the RTL-LUE model.

However, there still exist some limitations in this study. First of all, LAI is the core inputs for both the TL-LUE and RTL-LUE models, and the use of remote sensing LAI may induce uncertainties in parameter calibration and GPP validation (Zhou et al., 2016). In order to investigate the sensitivities of GPP performance to LAI inputs in the two models, the accuracy of GPP simulations from the MODIS LAI products (as shown in Table S4) are compared with the results from the GLASS LAI products. Results indicate that the GPP simulations from RTL-LUE also agree better with the EC GPP than the results of TL-LUE in all the 12 vegetation types, when using the MODIS LAI as the input. Similar to the previous studies (Liu et al., 2018; Xie et al., 2019), GPP simulated from the GLASS LAI has a better agreement with EC GPP than the results from the MODIS

LAI with much lower RMSE and bias, both for TL-LUE and RTL-LUE model. However, significant discrepancies can be found in the R^2 between the GPP simulations and the EC GPP among different vegetation types. The simulation results from the GLASS LAI still generally showed higher R^2 at forest sites, but showed lower R^2 at GRA, CRO, OSH, and WET sites. As a result, it can be concluded that although the RTL-LUE model can outperform the TL-LUE model both using GLASS and MODIS LAI products, different LAI products will certainly have significant impacts on the GPP simulation results both for the two models, with large discrepancies among different vegetation types. Besides, the cloud and atmospheric conditions induced abnormal variations in the LAI time series, and the mismatch of the spatial resolution of LAI products and the flux footprints may also lead to some uncertainties (Chen, 1999; Chu et al., 2021; He et al., 2013). LAI of a pixel from the GLASS product represents the mean value of the 1 km area, rather than the mean LAI of the unique vegetation types or regions measured by a flux tower. Further studies can be conducted using LAI products with high spatial resolutions and high accuracy in conjunction with flux footprints.

In addition, the EC sites in the FLUX2015 dataset with more than one year of valid half-hour data are all selected in this study. The neglect of the heterogeneous land cover of the flux sites may also induce uncertainties both in the parameterization and validation (Zhou et al., 2016). The low criteria are employed to select data because we want to verify the accuracy of the model as broadly as possible. Further research
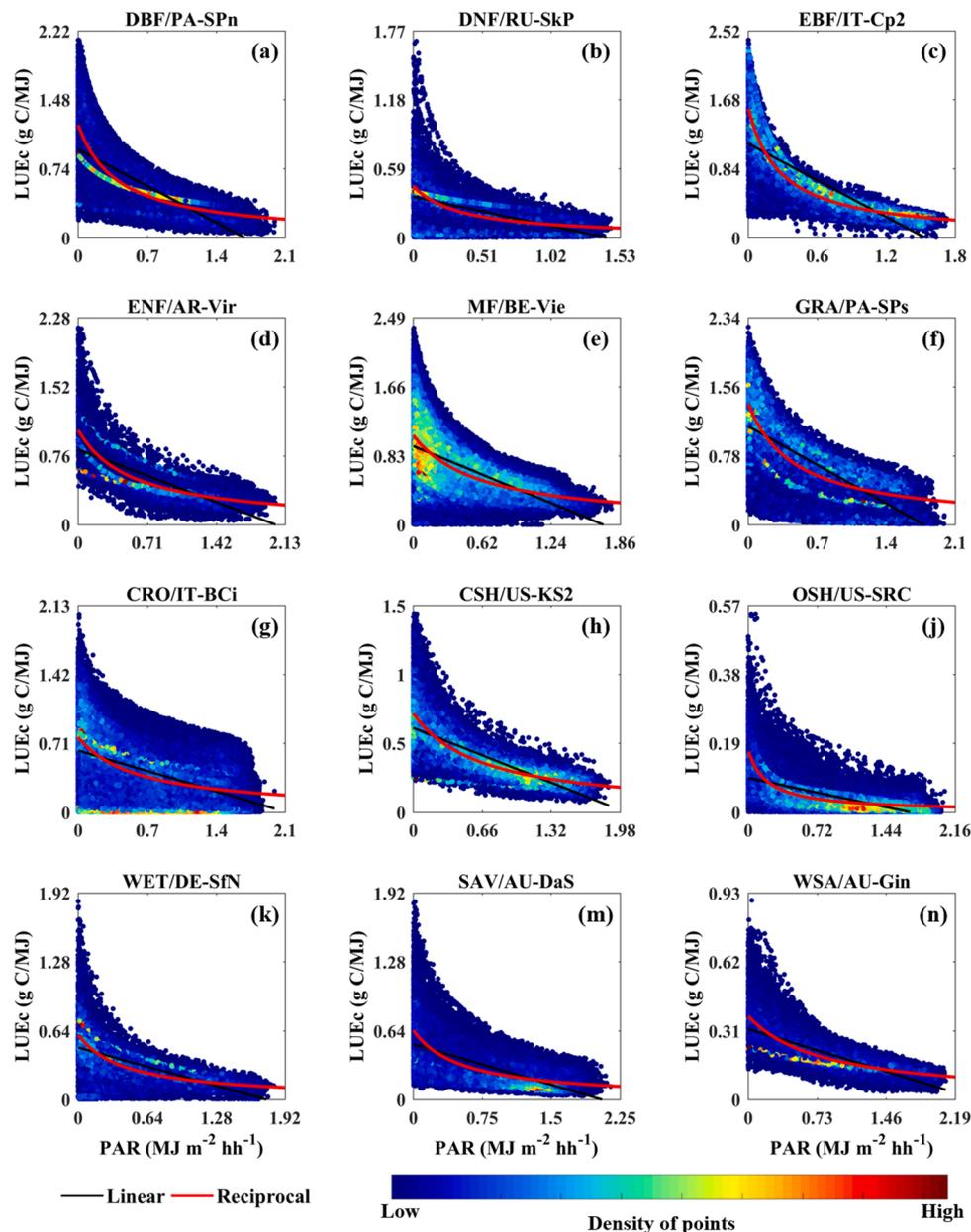
Figure 7. Comparison of the linear and reciprocal relationship between canopy LUE(LUEc=GPP/PAR) and PAR using site observations. The title of each subplot is named as "vegetation types/site name".

can be conducted to explore whether there are differences in the conclusions if the flux sites with very heterogeneous vegetation types are excluded. Furthermore, we assume that the discrepancies in LUE between sunlit and shaded leaves are mainly decided by the different light intensity they received, and the impacts of temperature, humidity, and nutrients are ignored. Actually, the sunlit leaves are supposed to have higher temperatures because they are directly exposed to the full sunlight, which will also impact the water vapor deficit at the leaf surface (Gates, 1964; Leuning et al., 1995; Miller, 1971). As a result, it is interesting to investigate if the temperature and humidity scalars for sunlit and shaded leaves can be calculated differently. These scalars used in the RTL-LUE model are the same as the MOD17 algorithm. The exclusion of soil water content, CO_2 fertilization, and nutrient conditions in optimizing LUE may have also limited the accuracy of GPP estimation to some extent (Chen et al., 2019a; Wang et al., 2020). Further efforts are needed to synthesizing the impacts of these factors on LUE.

5. Conclusion

In this study, a radiation-constrained two-leaf light use efficiency (RTL-LUE) model is developed to improve the simulation of GPP on the basis of a TL-LUE model. This new model assigns the same maximum LUE to both sunlit and shaded leaves, and the differences in LUE between them are represented by a scalar of radiation. The core parameters of TL-LUE and RTL-LUE models were optimized and the accuracies of GPP simulations by these two models were assessed, based on the measurements from globally distributed 169 EC sites. GPP simulations from the two models generally agree well with EC GPP, but consistent improvements can be observed in results from RTL-LUE (R^2=0.74, RMSE=358.81 g C m^{-2} year^{-1}) over TL-LUE (R^2=0.72, RMSE= 524.09 g C m^{-2} year^{-1}). The improvements are the largest at forest sites. GPP simulations from RTL-LUE show higher R^2 and lower RMSE and bias than those from TL-LUE either in all or individual vegetation types, for half-hour, 8-day, and yearly time scales. Besides, the diurnal and seasonal variations of GPP simulated by RTL-LUE also fit better with the EC

Table 6

Comparing the linear and reciprocal relationships between LUEc (GPP/PAR) and PAR based on site observations for different vegetation types.

Vegetation type [a]	Linear		Reciprocal		Difference		Percentage [b] (%)	
	R^2	RMSE [c]	R^2	RMSE [c]	R^2	RMSE [b]	R^2	RMSE [c]
DBF	0.13	0.35	0.15	0.34	0.02	-0.01	94.74	94.74
DNF	0.23	0.17	0.28	0.16	0.05	-0.01	1	1
EBF	0.57	0.18	0.64	0.16	0.07	-0.02	1	1
ENF	0.28	0.23	0.33	0.22	0.05	-0.01	1	1
MF	0.22	0.28	0.24	0.27	0.02	-0.01	1	1
GRA	0.19	0.23	0.23	0.22	0.04	-0.01	96.88	96.88
CRO	0.07	0.34	0.08	0.34	0.01	-0.00	1	1
CSH	0.53	0.14	0.58	0.13	0.05	-0.01	1	1
OSH	0.22	0.11	0.29	0.10	0.06	-0.01	1	1
WET	0.15	0.23	0.17	0.22	0.02	-0.01	1	1
SAV	0.25	0.19	0.28	0.18	0.03	-0.01	1	1
WSA	0.29	0.15	0.34	0.14	0.05	-0.01	1	1
All	0.27	0.23	0.23	0.24	0.04	-0.01	98.82	98.82

[a] The abbreviation of different vegetation types are the same as it in Table 1

[b] Percentage means the percentage of sites that the reciprocal relationship was better than linear to regress the LUEc=GPP/PAR and PAR, i.e., with a higher R^2 and lower RMSE

[c] unit of RMSE is g C m^{-2} hh^{-1}.
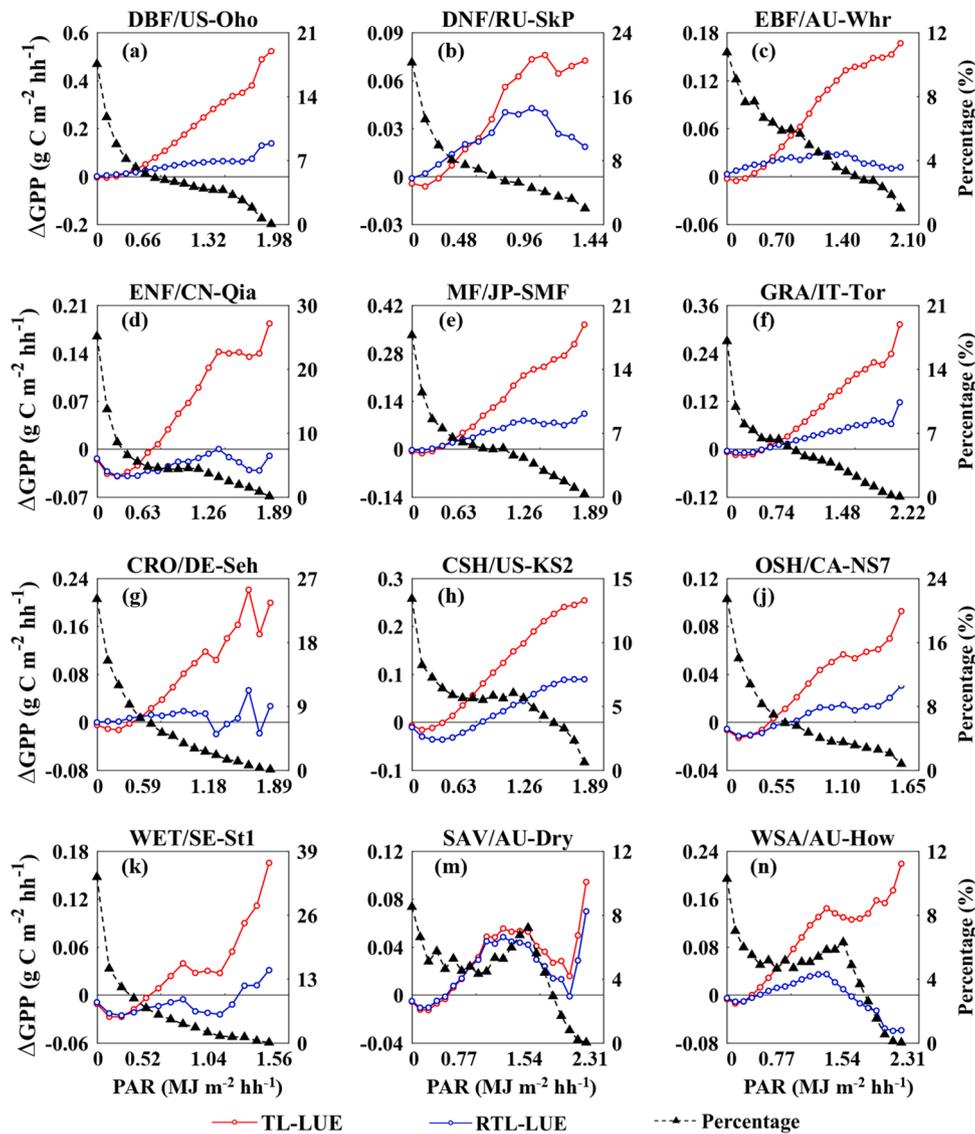
Figure 8. The sensitivity of GPP simulations to PAR for 12 specific sites with different vegetation types (ΔGPP = GPP$_{simulation}$ − GPP$_{EC}$, Percentage means the percentage of point numbers within the ranges of PAR). The title of each subplot is named as "vegetation types/site name".
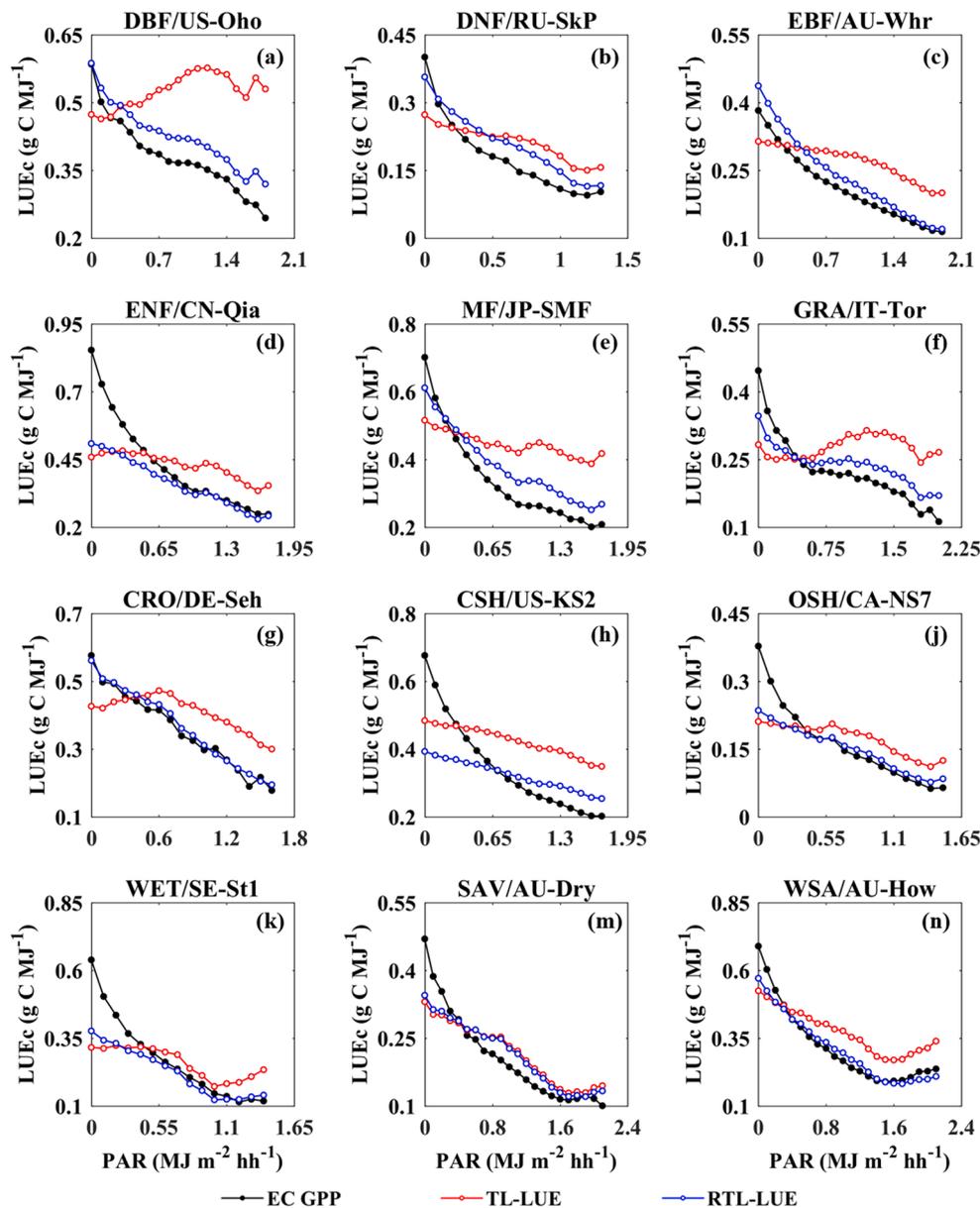
Figure 9. Comparison of the dependence of canopy light use efficiency (LUEc = GPP/PAR) on PAR averaged over 0.01 bins of PAR at 12 specific sites with different vegetation types. The title of each subplot is named as "vegetation types/site name".

observations than those by TL-LUE, because the overestimation at high incoming PAR (at noon and in peak growing season) by TL-LUE is significantly alleviated by the radiation scalar used in RTL-LUE. The optimized values of ε_{max}^{*} in the RTL-LUE model are generally lower than ε_{msh} and higher than ε_{msu} optimized in the TL-LUE model, and show similar variation with ε_{msh} among 12 vegetation types. The scatter plots of canopy LUE and PAR based on EC observations show that it is reasonable to use the reciprocal scalar of radiation to constrain LUE. Further statistics indicate that the RTL-LUE model showed a much lower sensitivity of error to PAR after considering the scalar of radiation. The overestimation of GPP in the TL-LUE model can be mainly explained by the optimized radiation-independent constant ε_{msh} and ε_{msu} values, which are only suitable for low-medium incoming PAR conditions that occurred most frequently and had the largest influence on the optimization of ε_{msh} and ε_{msu}.

This study highlights the importance of the radiation scalar in simulating GPP in LUE models even after the differentiation of LUE between sunlit and shaded leaf groups, because LUE would still vary within the same group and the difference in LUE between the two groups would also vary with radiation. We also demonstrate the excellent performance of the RTL-LUE model under most circumstances without differentiating the maximum LUE between sunlit and shaded leaves in order to minimize the number of parameters to be optimized. This seems to be a workable strategy as the small difference in leaf physiology between sunlit and shaded leaves would be superseded by the difference in light intensity on these two leaf groups. Further efforts in improving the RTL-LUE models may be directed towards the scalars of temperature and VPD and the possible differentiation of these scalars between sunlit and shaded leaves.

Declaration of Competing Interest

The authors declare that they have no known competing financial interests or personal relationships that could have appeared to influence the work reported in this paper.

Acknowledgments

Supplementary materials

Supplementary material associated with this article can be found, in the online version, at doi:10.1016/j.agrformet.2021.108546.

References

Beer, C., et al., 2010. Terrestrial gross carbon dioxide uptake: global distribution and covariation with climate. Science 329 (5993), 834–838.

Chen, B., et al., 2020. Importance of shaded leaf contribution to the total GPP of Canadian terrestrial ecosystems: evaluation of MODIS GPP. Journal of Geophysical Research: Biogeosciences 125 (10), e2020JG005917.

Chen, B., et al., 2019a. Including soil water stress in process-based ecosystem models by scaling down maximum carboxylation rate using accumulated soil water deficit. Agricultural and Forest Meteorology 276, 107649.

Chen, J., Liu, J., Cihlar, J., Goulden, M., 1999. Daily canopy photosynthesis model through temporal and spatial scaling for remote sensing applications. Ecological modelling 124 (2-3), 99–119.

Chen, J.M., 1999. Spatial scaling of a remotely sensed surface parameter by contexture. Remote Sensing of Environment 69 (1), 30–42.

Chen, J.M., et al., 2019b. Vegetation structural change since 1981 significantly enhanced the terrestrial carbon sink. Nature communications 10 (1), 1–7.

Chen, J.M., et al., 2012. Effects of foliage clumping on the estimation of global terrestrial gross primary productivity. Global Biogeochemical Cycles 26 (1).

Chu, D. et al., 2021. Long time-series NDVI reconstruction in cloud-prone regions via spatio-temporal tensor completion. arXiv preprint arXiv:2102.02603.

De Pury, D., Farquhar, G., 1997. Simple scaling of photosynthesis from leaves to canopies without the errors of big-leaf models. Plant, Cell & Environment 20 (5), 537–557.

Dong, J., et al., 2015. Comparison of four EVI-based models for estimating gross primary production of maize and soybean croplands and tallgrass prairie under severe drought. Remote Sensing of Environment 162, 154–168.

Duan, Q., Sorooshian, S., Gupta, V., 1992. Effective and efficient global optimization for conceptual rainfall-runoff models. Water resources research 28 (4), 1015–1031.

Falkowski, P., et al., 2000. The global carbon cycle: a test of our knowledge of earth as a system. science 290 (5490), 291–296.

Farquhar, G.D., von Caemmerer, S.v., Berry, J.A., 1980. A biochemical model of photosynthetic CO 2 assimilation in leaves of C 3 species. Planta 149 (1), 78–90.

Gates, D.M., 1964. Leaf temperature and transpiration 1. Agronomy Journal 56 (3), 273–277.

Guan, X., Shen, H., Li, X., Gan, W., Zhang, L., 2019. A long-term and comprehensive assessment of the urbanization-induced impacts on vegetation net primary productivity. The Science of the total environment 669, 342–352.

Haxeltine, A., Prentice, I., 1996. A general model for the light-use efficiency of primary production. Functional Ecology 551–561.

He, L., et al., 2018. Changes in the shadow: the shifting role of shaded leaves in global carbon and water cycles under climate change. Geophysical Research Letters 45 (10), 5052–5061.

He, M., et al., 2013. Development of a two-leaf light use efficiency model for improving the calculation of terrestrial gross primary productivity. Agricultural and Forest Meteorology 173, 28–39.

Hikosaka, K., 1996. Effects of leaf age, nitrogen nutrition and photon flux density on the organization of the photosynthetic apparatus in leaves of a vine (Ipomoea tricolor Cav.) grown horizontally to avoid mutual shading of leaves. Planta 198 (1), 144–150.

Hunt Jr, E.R., Running, S.W., 1992. Simulated dry matter yields for aspen and spruce stands in the North American boreal forest. Canadian journal of remote sensing 18 (3), 126–133.

Koyama, K., Kikuzawa, K., 2010. Geometrical similarity analysis of photosynthetic light response curves, light saturation and light use efficiency. Oecologia 164 (1), 53–63.

Leuning, R., Kelliher, F.M., De Pury, D., Schulze, E.D., 1995. Leaf nitrogen, photosynthesis, conductance and transpiration: scaling from leaves to canopies. Plant, Cell & Environment 18 (10), 1183–1200.

Leverenz, J.W., 1987. Chlorophyll content and the light response curve of shade-adapted conifer needles. Physiologia Plantarum 71 (1), 20–29.

Liu, J., Chen, J., Cihlar, J., Park, W., 1997. A process-based boreal ecosystem productivity simulator using remote sensing inputs. Remote sensing of environment 62 (2), 158–175.

Liu, Y., et al., 2018. Satellite-derived LAI products exhibit large discrepancies and can lead to substantial uncertainty in simulated carbon and water fluxes. Remote Sensing of Environment 206, 174–188.

Marcott, S.A., et al., 2014. Centennial-scale changes in the global carbon cycle during the last deglaciation. Nature 514 (7524), 616–619.

Marshall, M., Tu, K., Brown, J., 2018. Optimizing a remote sensing production efficiency model for macro-scale GPP and yield estimation in agroecosystems. Remote sensing of environment 217, 258–271.

Mattos, E.M., Binkley, D., Campoe, O.C., Alvares, C.A., Stape, J.L., 2020. Variation in canopy structure, leaf area, light interception and light use efficiency among Eucalyptus clones. Forest Ecology and Management 463, 118038.

McCallum, I., et al., 2013. Improved light and temperature responses for light-use-efficiency-based GPP models. Biogeosciences 10 (10), 6577–6590.

Mercado, L.M., et al., 2009. Impact of changes in diffuse radiation on the global land carbon sink. Nature 458 (7241), 1014–1017.

Miller, P.C., 1971. Sampling to estimate mean leaf temperatures and transpiration rates in vegetation canopies. Ecology 52 (5), 885–889.

Myneni, R., Knyazikhin, Y., Park, T., 2015. MOD15A2H MODIS/terra leaf area index/FPAR 8-Day L4 global 500m SIN grid V006. NASA EOSDIS Land Processes DAAC.

Ogren, E., 1993. Convexity of the photosynthetic light-response curve in relation to intensity and direction of light during growth. Plant physiology 101 (3), 1013–1019.

Oliphant, A., et al., 2011. The role of sky conditions on gross primary production in a mixed deciduous forest. Agricultural and Forest Meteorology 151 (7), 781–791.

Pastorello, G., et al., 2017. A new data set to keep a sharper eye on land-air exchanges. Eos, Transactions American Geophysical Union (Online) 98 (8).

Pastorello, G., et al., 2020. The FLUXNET2015 dataset and the ONEFlux processing pipeline for eddy covariance data. Scientific data 7 (1), 1–27.

Perkins, R.G., Mouget, J.-L., Lefebvre, S., Lavaud, J., 2006. Light response curve methodology and possible implications in the application of chlorophyll fluorescence to benthic diatoms. Marine Biology 149 (4), 703–712.

Potter, C.S., et al., 1993. Terrestrial ecosystem production: a process model based on global satellite and surface data. Global Biogeochemical Cycles 7 (4), 811–841.

Propastin, P., Ibrom, A., Knohl, A., Erasmi, S., 2012. Effects of canopy photosynthesis saturation on the estimation of gross primary productivity from MODIS data in a tropical forest. Remote Sensing of Environment 121, 252–260.

Rap, A., et al., 2018. Enhanced global primary production by biogenic aerosol via diffuse radiation fertilization. Nature Geoscience 11 (9), 640–644.

Reichstein, M., et al., 2005. On the separation of net ecosystem exchange into assimilation and ecosystem respiration: review and improved algorithm. Global change biology 11 (9), 1424–1439.

Running, S.W., et al., 2004. A continuous satellite-derived measure of global terrestrial primary production. Bioscience 54 (6), 547–560.

Sinclair, T., Horie, T., 1989. Leaf nitrogen, photosynthesis, and crop radiation use efficiency: a review. Crop science 29 (1), 90–98.

Wang, S., et al., 2015. Improving the light use efficiency model for simulating terrestrial vegetation gross primary production by the inclusion of diffuse radiation across ecosystems in China. Ecological Complexity 23, 1–13.

Wang, S., et al., 2020. Recent global decline of CO2 fertilization effects on vegetation photosynthesis. Science 370 (6522), 1295–1300.

Wang, Y.-P., Leuning, R., 1998. A two-leaf model for canopy conductance, photosynthesis and partitioning of available energy I:: Model description and comparison with a multi-layered model. Agricultural and Forest Meteorology 91 (1-2), 89–111.

Xia, J., et al., 2015. Joint control of terrestrial gross primary productivity by plant phenology and physiology. Proceedings of the National Academy of Sciences 112 (9), 2788–2793.

Xiao, J., et al., 2010. A continuous measure of gross primary production for the conterminous United States derived from MODIS and AmeriFlux data. Remote sensing of environment 114 (3), 576–591.

Xiao, X., et al., 2004. Satellite-based modeling of gross primary production in an evergreen needleleaf forest. Remote sensing of environment 89 (4), 519–534.

Xiao, Z., Liang, S., Jiang, B., 2017. Evaluation of four long time-series global leaf area index products. Agricultural and Forest Meteorology 246, 218–230.

Xiao, Z., et al., 2016. Long-time-series global land surface satellite leaf area index product derived from MODIS and AVHRR surface reflectance. IEEE Transactions on Geoscience and Remote Sensing 54 (9), 5301–5318.

Xie, X., et al., 2019. Assessment of five satellite-derived LAI datasets for GPP estimations through ecosystem models. The Science of the total environment 690, 1120–1130.

Yang, J., et al., 2013. The role of satellite remote sensing in climate change studies. Nature climate change 3 (10), 875–883.

Yuan, W., et al., 2014. Global comparison of light use efficiency models for simulating terrestrial vegetation gross primary production based on the LaThuile database. Agricultural and Forest Meteorology 192-193, 108–120.

Yuan, W., et al., 2007. Deriving a light use efficiency model from eddy covariance flux data for predicting daily gross primary production across biomes. Agricultural and Forest Meteorology 143 (3-4), 189–207.

Zhang, F., et al., 2012. Evaluating spatial and temporal patterns of MODIS GPP over the conterminous US against flux measurements and a process model. Remote Sensing of Environment 124, 717–729.

Zhang, L.-X., Zhou, D.-C., Fan, J.-W., Hu, Z.-M., 2015. Comparison of four light use efficiency models for estimating terrestrial gross primary production. Ecological Modelling 300, 30–39.

Zhang, M., et al., 2011. Effects of cloudiness change on net ecosystem exchange, light use efficiency, and water use efficiency in typical ecosystems of China. Agricultural and Forest Meteorology 151 (7), 803–816.

Zhang, Y., et al., 2017. A global moderate resolution dataset of gross primary production of vegetation for 2000–2016. Scientific data 4 (1), 1–13.

Zheng, T., et al., 2017. Inverting the maximum carboxylation rate (Vcmax) from the sunlit leaf photosynthesis rate derived from measured light response curves at tower flux sites. Agricultural and Forest Meteorology 236, 48–66.

Zhou, Y., et al., 2016. Global parameterization and validation of a two-leaf light use efficiency model for predicting gross primary production across FLUXNET sites. Journal of Geophysical Research: Biogeosciences 121 (4), 1045–1072.